NASA TECHNICAL MEMORANDUM

NASA TM X-71492

NASA TM X-71492

LOW-HIGH JUNCTION THEORY APPLIED TO SOLAR CELLS

by Michael P. Godlewski, Cosmo R. Baraona,
and Henry W. Brandhorst, Jr.
Lewis Research Center 44135
Cleveland, Ohio

TECHNICAL PAPER presented at
Tenth Photovoltaic Specialists Conference sponsored by
the Institute of Electrical and Electronics Engineers
Palo Aito, California, November 13-15, 1973

LOW-HIGH JUNCTION THEORY APPLIED TO SOLAR CELLS

by Michael P. Godlewski, Cosmo R. Baraona,
and Henry W. Brandhorst, Jr.

National Aeronautics and Space Administration
Lewis Research Center
Cleveland, Ohio

SUMMARY

Recent use of alloying techniques for rear contact formation has yielded a new kind of silicon solar cell, the back surface field (BSF) cell, with abnormally high open circuit voltage (V_{oc}) and improved radiation resistance. Several analytical models for V_{oc} based on the reverse saturation current are formulated to explain these observations. The zero SRV case of the conventional cell model, the drift field model, and the low-high junction (LHJ) model can predict the experimental trends. The LHJ model applies the theory of the low-high junction and is considered to reflect a more realistic view of cell fabrication. This model can predict the experimental trends observed for BSF cells. Detailed descriptions and derivations for the models are included. The correspondences between them are discussed. This modeling suggests that the meaning of minority carrier diffusion length measured in BSF cells be reexamined.

TABLE OF SYMBOLS

D	minority carrier diffusion coefficient, cm^2/sec
E	electric field strength, volt/cm
G	minority carrier generation rate, sec^{-1}
I_{sc}	short circuit current density, amp/cm^2
I_o	diode saturation current density, amp/cm^2
J	minority carrier current density, amp/cm^2
K	damage constant for 1 MeV electrons, $particle^{-1}$
k	Boltzman constant, 1.38×10^{-23} joules/K
L	minority carrier diffusion length, cm
n	minority carrier concentration, cm^{-3}
Δn, Δp	excess electron or hole concentration, cm^{-3}
n_i	intrinsic carrier concentration, cm^{-3}
N_D	donor concentration in n-type material, cm^{-3}
N_A, N_{A+}	acceptor concentration in p, p+ material, cm^{-3}
q	electronic charge, 1.6×10^{-19} coulombs
R	minority carrier recombination rate, sec^{-1}
s	surface recombination velocity, cm/sec
S	normalized surface recombination velocity for low-high junction model, dimensionless
t	total solar cell thickness, cm
T	temperature, kelvin
V_{oc}	open circuit voltage, volts
W	region thickness, cm
x	arbitrary distance into the cell, cm
x_j	depth of metallurgical junction, cm
X	subregion boundary plane location, cm
μ	minority carrier mobility, $cm^2/volt\ sec$
τ	minority carrier lifetime, sec
ϕ	fluence of 1 MeV electrons, cm^{-2}
ψ	equilibrium barrier potential of the low-high junction, volts

Subscripts

p	associated with p-type region or with minority carrier electrons
p+	associated with p+-type region
n	associated with n-type region or with minority carrier holes
n+	associated with n+-type region

INTRODUCTION

Recent efforts to improve the performance of silicon solar cells have resulted in an increased open circuit voltage (V_{oc}) for 10 ohm-cm silicon material. For years the V_{oc} of the 10 ohm-cm silicon cell was fixed at about 0.55 volts. However the use of an alloying fabrication technique (1) for rear contact formation has resulted in the back-surface field (BSF) cell having voltages as high as 0.58 volts. In addition, improvements in short circuit current, efficiency and fill factor have also been observed. Unlike the conventional 10 ohm-cm cell, the V_{oc} of the BSF cell appears to be independent of cell thickness at least over the thickness range of 100 to 400 micrometers. These improvements in cell performance are directly attributed to the presence of a heavily doped p-type layer (referred to as the p+ layer) formed during rear contact fabrication. Measurements of the effective diffusion length of these cells using various techniques have produced uncertain information. In some cases the effective diffusion lengths are in excess of values measured for conventional cells.

Analytical modeling for the BSF cell has not received as much attention as the experimental work. Thus the purpose of this paper is to present calculations of V_{oc} based on conventional, drift field, and low-high junction one dimensional solar cell models and to test these calculated results against the experimental data. The model for the conventional cell assumes an arbitrary front and back surface recombination velocity (SRV). This model has four limiting cases: 1) the infinite SRV case, 2) the zero SRV case, 3) the SRV equals diffusion velocity case, and 4) the infinitely thick cell. The drift field model for V_{oc} is based on the same assumptions and boundary conditions as Wolf's drift field model used for the calculation of collection efficiency (2). The new model to be

proposed here is the low-high junction (LHJ) model. The requirement for a LHJ rear contact structure (p-p+) in the BSF cell results in boundary conditions that reflect the minority carrier blocking properties of the LHJ first reported by J. B. Gunn (3). The LHJ model presented here differs from that derived by Sutton and Whittier (4) by neglecting space charge recombination effects. However this work extends the work of ref. 4 by including the p+ region geometry factor.

Although LHJ effects are well-known and have been applied to the modeling and analysis of semiconductor rectifiers (5), this paper represents a first attempt at applying this model to photovoltaic energy converters.

The approach taken in the modeling is to relate the V_{oc} to the diode saturation current (I_o) and short circuit current (I_{sc}). Expressions for I_o are derived assuming boundary conditions for low injection minority carrier transport with boundary conditions appropriate to each model. The performance of all the models and cases is compared with the experimental V_{oc} versus thickness data. Finally, the radiation degradation behavior of V_{oc} is calculated using the LHJ model.

THEORY

If it is assumed that the current transport in a solar cell is dominated by minority carrier diffusion processes, then the open circuit voltage (V_{oc}) can be related to the short circuit current (I_{sc}) and the diode saturation current (I_o) by the following simple expression

$$V_{oc} = \frac{kT}{q} \ln\left(\frac{I_{sc}}{I_o} + 1\right) \tag{1}$$

Hence an analysis of the V_{oc} can be made for the conventional, drift field, and low-high junction models of the solar cell using expressions for I_o which reflect the cell structure and properties unique to each model. These expressions are given below. Calculations were made using a high speed digital computer and a programmable desk top calculator. All calculations were made for short circuit density of about 40 ma/cm^2 and a diffused region saturation current (I_{o_n}) equal to 1.2×10^{-14} amp/cm^2.

Conventional I_o Expressions

A common view of the conventional n on p solar cell structure is one in which the p-base dopant and properties are uniform, the device dimensions are finite, and contact effects are described by the surface recombination velocity (SRV). The I_o for this general case has been derived by McKelvey (6). This expression is given by equation (2a) for the n and p regions.

$$I_o = \frac{qn_i^2 D_p}{N_D}\left\{\frac{\frac{s_f L_p}{D_p} + \tanh\frac{W_n}{L_p}}{1 + \frac{s_f L_p}{D_p}\tanh\frac{W_n}{L_p}}\right\}\frac{1}{L_p} + \frac{qn_i^2 D_n}{N_A}\left\{\frac{\frac{s_r L_n}{D_n} + \tanh\frac{W_p}{L_n}}{1 + \frac{s_r L_n}{D_n}\tanh\frac{W_p}{L_n}}\right\}\frac{1}{L_n} \tag{2a}$$

The SRV is represented by s, and L is the bulk diffusion length. The other parameters have their usual meaning. Note that the product of the diffusion length (L_n or L_p) with the reciprocal of the bracketed terms defines an "effective" device diffusion length. This equation however reduces to the following approximate forms.

1) Infinite SRV Case. When s_r and s_f are very large as would be the case for ohmic contacts, equation (2a) reduces to the familiar hyperbolic cotangent form.

$$I_o = \frac{qn_i^2 D_p}{N_D L_p}\coth\frac{W_n}{L_p} + \frac{qn_i^2 D_n}{N_A L_n}\coth\frac{W_p}{L_n} \tag{2b}$$

This case gives a reasonable description of the base region of the conventional cell structure.

2) Zero SRV Case. If the SRV's are assumed to be zero, (2a) reduces to a second form now containing the hyperbolic tangent geometry factor.

$$I_o = \frac{qn_i^2 D_p}{N_D L_p}\tanh\frac{W_n}{L_p} + \frac{qn_i^2 D_n}{N_A L_n}\tanh\frac{W_p}{L_n} \tag{2c}$$

This case implies non-ohmic contacts and does not reflect the practical solar cell.

3) Diffusion Velocity Case. If the SRV for the front and rear contacts are equal to the minority carrier diffusion velocities (D/L) in each base region, the bracketed terms of equation (2a) reduce to unity. This approximate I_o is identical to the infinite base case given below.

4) Infinite Base Case. When the base region thicknesses are much greater than the bulk diffusion lengths, the bracketed terms in equation (2a) again reduce to unity. The resultant I_o given by equation (2d) is the well-known expression derived by Shockley (7).

$$I_o = \frac{qn_i^2 D_p}{N_D L_p} + \frac{qn_i^2 D_n}{N_A L_n} \tag{2d}$$

This case and the preceding case predict the I_o to be independent of base region thickness.

Drift Field Model I_o

Practical solar cells are fabricated by diffusion and alloying processes which usually result in regions having significant non-uniform impurity distributions. It is easily shown that such distributions give rise to an electric field which can significantly influence minority carrier transport in those regions. Kleinman (8) and Wolf (2) have calculated the cell I_{sc} using an expression for the collection efficiency which contains drift field effects. The cell was mathematically divided into subregions which can be assigned separate material properties and dimensions. For example Wolf used a four layer model in which exponential impurity distributions could be assigned to each region. The important features of this model are that the minority carrier density and the current density are continuous at the subregion boundary. The I_o for this structure has been derived (9) and includes not only finite geometry and contact effects, but also the effect of subregion drift fields. The p-base component of the n on

p solar cell containing a drift field only in a thin region in front of the rear contact is given by equation (3). The p-type base subregion nearest the junction is uniformly doped and therefore field free.

$$I_{o_p} = \frac{qn_i^2}{N_A}\frac{D_{n1}}{L_{n1}}\left\{\frac{c-1}{c+1}\right\} \qquad (3)$$

where

$$c = e^{2\frac{(X-x_j)}{L_{n1}}}\left\{\frac{-\left(\frac{1}{L_{n1}}-\gamma A_2\right)\left(\frac{R-A_2}{R-B_2}\right)e^{2G_{n2}(W-X)}+\left(\frac{1}{L_{n1}}+\gamma B_2\right)}{\left(\frac{1}{L_{n1}}-\gamma A_2\right)\left(\frac{R-A_2}{R-B_2}\right)e^{2G_{n2}(W-X)}-\left(\frac{1}{L_{n1}}-\gamma B_2\right)}\right\}$$

$$A_2 = \frac{qE_2}{2kT} - \left\{\left(\frac{qE_2}{2kT}\right)^2 + \frac{1}{L_{n2}^2}\right\}^{1/2} \equiv F_{n2} - G_{n2}$$

$$B_2 = F_{n2} + G_{n2}$$

$$\gamma = D_{n2}/D_{n1}$$

$$R = \frac{qE_2}{kT} + \frac{s}{D_{n2}}$$

A similar expression is written for the n-type diffused region with the appropriate change in subscripts and by assuming an erfc donor distribution. The drift field region is nearest the junction for this case. It can be seen that equation (3) will reduce to the general SRV case given by equation (2a) if a single layer, field free model is assumed.

Low-High Junction (LHJ) Model I_o

For the LHJ model, the subregion boundary, unlike the drift field model, represents an abrupt transition between the thick, lightly-doped p-region (i.e., subregion nearest the junction) and the thin heavily-doped p+ region. Both regions are assumed uniform in dopant and materials properties. It has been shown by Gunn that this junction has the unique property of preventing excess minority carriers in the p-base from entering the p+ region. Majority carriers pass freely across this junction. The minority carrier concentrations at the space charge region edges depend on the barrier potential (v) associated with the low-high junction as shown in equation (4a)

$$n_p = n_{p+} \exp\frac{q\psi}{kT} \qquad (4a)$$

In addition, the diffusion currents at the p+ and p region space charge edges are proportional to the gradients of the minority carrier densities there, and given by equation (4b)

$$qD_p \nabla n_p = qD_{p+} \nabla n_{p+} \qquad (4b)$$

Equation (4a) represents a subregion boundary condition which differs significantly from that assumed in the drift field model. Recombination effects and thickness of the LHJ space charge region are assumed negligible. The I_o using this model is derived in detail in the Appendix. The result for the p-side is given by equation (5) where t is the cell total thickness

$$I_{o_p} = \frac{qn_i^2 D_n}{N_A L_p}\left\{\frac{S + \tanh\frac{W_p}{L_p}}{1 + S\tanh\frac{W_p}{L_p}}\right\} \qquad (5)$$

where

$$S = \frac{N_A}{N_{A+}}\frac{D_{p+}}{D_p}\frac{L_p}{L_{p+}}\left\{\frac{\frac{s_r L_{p+}}{D_{p+}} + \tanh\frac{W_{p+}}{L_{p+}}}{1 + \frac{s_r L_{p+}}{D_{p+}}\tanh\frac{W_{p+}}{L_{p+}}}\right\}$$

The parameter S is defined as a normalized surface recombination velocity. It contains the LHJ barrier factor (N_A/N_{A+}) and the mobility and diffusion length ratios for the p and p+ region. S also contains a geometry factor for the p+ region, the SRV for the metal-p+ contact (s_r), and the p+ region thickness (W_{p+}). The total I_o must include the n-base component I_{o_n}. In the simplest case I_{o_n} is described by the drift field model given by equation (2). However for the range of variables considered here, I_{o_p} is always significantly greater than I_{o_n} for 10 ohm-cm material. Therefore I_{o_n} is neglected. However the importance of I_{o_n} and its effect on the performance of low resistivity and deep diffused cells is recognized.

REVIEW OF EXPERIMENTAL DATA

Published measurements on the high voltage (BSF) 10 ohm-cm solar cell are assembled here to provide a comparison with the theoretical predictions. The data, shown in figure 1, are grouped into two categories as follows: dependence of V_{oc} on cell thickness (1) and the response of V_{oc} to 1 MeV electron exposure (1, 10). The data of ref. 1 for the high voltage cell is shown in fig. 1a. Voltages as high as 0.58 v are measured and are approximately independent of cell thickness in the 100 to 300 micron range. V_{oc} variations of ± 5 mv at each thickness are not unreasonable. More recent unpublished data suggest that constant voltages as high as 0.60 volts are achievable. These data are in striking contrast to those shown for the conventional cell, where thinner cells have lower voltages. Apparently the only difference in the fabrication between the high voltage and conventional 10 ohm-cm cells is the additional alloying and/or diffusion and sintering associated with the rear contact of the high voltage cells. The radiation behavior (1) of various thicknesses of high voltage cell is shown in fig. 1b. Also shown are data for conventional cells of 150 and 300 micron thickness. The initial voltages are higher for the high voltage cell compared to the conventional cell of comparable thickness. In addition the high voltage cells maintain a higher voltage for larger fluences than do the conventional cells. Furthermore the thin high voltage cell maintains a superiority over the thick high voltage cell. At high fluences the magnitude of the voltage and the radiation degradation rate of all high voltage cells are the same as for the conventional cell. Also shown in the figure are unpublished data (10) for a 100 um high voltage cell measured by JPL.

RESULTS

A study of the open circuit voltage dependence on cell structure has been made using equation (1) and equations (2), (3), and (5).

Conventional Model

Figure 2 shows the dependence of V_{oc} on p-base diffusion length for the infinite base case where the requirement is that $W_p \gg L_p$. As can be seen voltages in excess of 0.590 volts are predicted providing the p-base diffusion length is greater than 1000 micrometers. This cell would be at least 0.3 cm thick in order to obey the cell thickness/diffusion length requirement. Because the model assumes an infinite (> 0.3 cm) thickness at all diffusion lengths, there is of course no V_{oc} dependence on thickness.

Voltages calculated for a range of cell thicknesses and p-base diffusion lengths using the finite width model are shown in fig. 3. The dotted, solid, and dashed lines represent calculations for the infinite SRV, the zero SRV, and the special case where the SRV is equal to the diffusion velocity (D/L), respectively. Voltages that are independent of cell thickness are predicted only for the latter case. For very thick cells and a specified diffusion length, all cases predict voltages that are approaching the limiting values of the infinite width case. This is not unexpected since the further away the rear contact is from the junction the less it will influence the minority carrier distribution in the p-base. As the cell becomes thinner, the predicted voltage trends become very different. It is seen that the zero SRV case predicts voltages for thin cells that are well in excess of those predicted by the other two cases. In addition only the zero SRV case will predict voltages above 0.58 volts provided the p-base diffusion length is substantially greater than 200 μm.

Drift Field Model

The results of the voltage calculations for the drift field model are shown in figs. 4 and 5. A 0.5 μm thick p+ region in which an exponential acceptor concentration profile exists was assumed. For the results shown in fig. 4, the p+ region diffusion length was assumed to be 1.0 μm. It can be seen that the magnitude of the voltage depends on cell thickness and p-base diffusion length. Below 0.54 volt (i.e., approximately 200 micrometer diffusion length) the V_{oc} is nearly independent of cell thickness. Above 0.54 volts the voltage increases with increasing cell thickness similar to the infinite SRV case.

Figure 5 shows the variations of the voltage for values of p+ region diffusion length between 1 and about 220 μm. Calculations were made for p region diffusion lengths of 50, 200, and 600 μm. The p+ region width is again 0.5 μm. As shown, the diffusion lengths associated with both regions control the magnitude of the voltage and its dependence on thickness. Large values of p+ region diffusion lengths are necessary to produce high voltages in thin cells. The voltages predicted for cells where the p-base diffusion length is much smaller than the base thickness are identical to those shown in fig. 2, the infinite base case.

Low-High Junction Model

The results of voltage calculations using the low-high junction model are shown in fig. 6 for a range of p-base diffusion lengths. In practice, there is a 20 mv spread in voltage reflecting the actual 7 to 14 ohm-cm resistivity variation for nominal 10 ohm-cm material. Silicon in this resistivity range is called nominal 10 ohm-cm. A uniform p+ region acceptor concentration of $1.3\times10^{19}/cm^3$ was assumed yielding a N_p/N_{p+} ratio of 10^{-4}. The p+ region thickness and diffusion length are 0.5 μm and 1.0 μm respectively. Contrary to the drift field model, increases in the p+ region diffusion length up to 200 μm had no influence on the V_{oc}. The voltages for thick cells as asymptotically approach those of the infinite base case since $W/L \gg 1$. For the conditions assumed, the shape and magnitude of the V_{oc}/thickness curves are identical to those calculated for the zero SRV case. Thus, the zero SRV case, can be used, as an approximation to the LHJ model, to calculate cell V_{oc} with p-region diffusion length as the only variable. As in the previous models, the magnitude of the voltage is determined primarily by the p-base diffusion length which in itself yields limited information. In the LHJ model the parameter S, which incorporates properties of the LHJ and the p regions, assumes major importance in determining cell performance.

Figure 7 shows a plot of the voltage against the magnitude of the normalized surface recombination velocity S defined by equation (5b). The calculations are made for several values of cell thickness for a p-base diffusion length of 574 μm. This figure shows clearly the influence of S on the magnitude of the voltage. For reference, the curve of figure 6 corresponding to the 600 μm diffusion length has an S equal to about 10^{-2}. For small values of S (less than unity), the voltage asymptotically approaches the values predicted by the zero SRV case shown in fig. 3. For large values of S, the V_{oc} approaches that predicted by the infinite SRV case of fig. 2. Thus fig. 7 shows graphically the manner in which the LHJ model reduces to both the zero SRV and infinite SRV models. For intermediate values of S in the range of 0.1 to 10, the voltage varies greatly between the two limiting cases. For S equal to unity, the voltage is independent of cell thickness and equal in magnitude to that predicted by the infinite width case.

Figure 8 shows the calculated voltage response to 1 MeV electron exposure. Response is calculated using the LHJ model for cells of various thickness. Calculations for the conventional cell of 100 and 400 μm thickness using the infinite SRV case is also shown. An initial p-base diffusion length of 400 μm is assumed for all cells. The voltage degradation is simulated by assuming that radiation damage alters the diffusion length through lifetime degradation. The diffusion length in the I_o equations is replaced by the following expression containing the radiation damage coefficient (K) and the initial diffusion length ($L_p(0)$):

$$\frac{1}{L_p^2(\Phi)} = \frac{1}{L_p^2(0)} + K\Phi \qquad (6)$$

Φ is the electron fluence and K is equal to 9×10^{-11} (electrons^{-1}) (11) for 10 ohm-cm material. At zero fluence the thin high voltage cells have higher voltages compared to the thick cells. This superiority is maintained to about 1×10^{15} e/cm^2. Beyond this all cells degrade at the same rate as the conventional cells.

DISCUSSION

Based on the above data, the infinite SRV case can explain the experimental trends of the conventional cell. As will be discussed below, the trends of the BSF cell are predicted using either the zero SRV case, the drift field model, or the LHJ model. However in all cases the "goodness of fit" is critically dependent on the magnitude of the bulk diffusion length used in the calculations. These diffusion lengths are not in agreement with those determined by experiment. Some reasons for this will be discussed.

Comparison of fig. 1a and fig. 3 shows that the infinite SRV case predicts the correct V_{oc} thickness trend for conventional cells. However the magnitude of the voltages for cells of different thicknesses cannot be predicted using a single value for the p-base diffusion length. The voltages for thin cells are predicted only for a diffusion length that is lower than for thick cells. For example, from fig. 1a, conventional cell voltages of 0.55 and 0.50 V are obtained for cell thicknesses of 300 and 100 μm respectively. Calculations using the infinite SRV model require bulk diffusion lengths of 300 and <50 μm respectively for these two cases. Cell measurements also indicate a reduction in diffusion length. The mechanism of this apparent reduction in diffusion length is not understood. It is possible that reductions in diffusion length are effected through impurity introduction during processing or by cell geometry changes.

Of more present interest are the voltages observed in the BSF cells. It is not possible to predict either the magnitude of the voltage or its trend with thickness for BSF cells using the infinite SRV case. The diffusion velocity case yields voltages above 0.58 V only if the p-base diffusion length is greater than 600 μm. In this case the voltages are independent of cell thickness. Also, the zero SRV case yields voltages above 0.58 V for diffusion lengths above 300 μm depending on cell thickness. The thicker the cell, the greater the necessary diffusion length. However these cases provide little information which is traceable to fabrication processes about the influence of cell structure properties on cell performance. Because of this, these cases will not be considered further.

The drift field model and the LHJ model also predict high voltages provided the W/L ratio of the p-base is less than unity. It should be noted that the drift field model approaches the voltage/thickness trend of the zero SRV case of the LHJ case only for high p^+ region diffusion lengths. In addition, these models both contain parameters relating to controllable cell fabrication features, such as p^+ region width and dopant concentrations, as well as carrier mobility and lifetime. As shown in figs. 5 and 7, these features can significantly influence calculated cell performance. Cases of observed independence of cell voltage on thickness are predicted by both these models. For the drift field model, the voltages will be nearly independent of cell thickness only for a particular value of p^+-region L which is about 2.5 μm for the 0.58 V case. The LHJ model can predict the experimental V_{oc}/thickness trends by applying one of the following approximations to equation (5):

1. $W_p \gg L_p$
2. $S = 1$
3. Diffusion length dependent on cell thickness.

The first approximation is trivial and yields the infinite base case. The BSF cells do not physically conform to this case. The second approximation, however, imposes specific relationships between certain cell properties. Equation (5b) for S can be reduced to equation (6) by assuming an ohmic contact to the p^+ region

$$S = \frac{N_A}{N_{A^+}} \frac{D_{p^+}}{D_p} \frac{L_p}{L_{p^+}} \coth \frac{W}{L}_{p^+} \qquad (6)$$

For S = 1, an appropriate relationship must be established between the p^+ region geometry, the diffusion velocities (D/L), and the LHJ barrier height (N_A/N_{A^+}). It is easily seen that there is no unique set of parameters which satisfies the condition. Therefore the S = 1 approximation would seem to necessitate a difficult interaction and/or counterbalancing of multiple cell parameters.

Examination of fig. 6 suggests that if a line corresponding to 0.58 volts, for example, were drawn parallel to the thickness axis, a unique value of diffusion length would correspond to each cell thickness. Using this method, a 150 μm thick cell would require a 300 μm diffusion length while a 500 μm thick cell would require a 500 μm diffusion length.

This trend of decreasing diffusion length with decreasing thickness is also observed in conventional cells as shown previously. Diffusion length measurements of Iles (12) on wafers ranging from 400 μm to several centimeters thick also suggest that diffusion length does indeed decrease monotonically as sample thickness decreases. The measured L varied from 200 μm for the 400 μm thick wafers to over 1000 μm for the very thick samples. All samples had ohmic contacts. No data presently exists for samples having "zero SRV"-like contacts as might be expected from a high voltage (BSF) cell rear contact. Therefore, from the trends seen in cells, a decrease of diffusion length with decreasing cell thickness appears to be reasonable, although no mechanism has been advanced as yet to rationalize the effect.

The requirement that high voltage cells have diffusion lengths that are substantially larger than the 200 μm measured for conventional cells also is of concern. However, in addition to the experimental evidence of Iles (12) that long diffusion lengths exist, other theoretical and experimental bases can be found in the literature. The published work by Zimmerman (13) suggests that the LHJ causes an excess minority carrier distribution in the p-base that differs significantly from the simple exponential profile that occurs in a conventional cell geometry. Therefore, it is suggested that methods of measuring diffusion length that rely on semi-infinite cell dimensions and/or ohmic contacts, although used on the LHJ structure, cannot be in the usual straightforward manner to yield the bulk diffusion length when a LHJ is present. In addition there is some experimental evidence from the work on epitaxial structures (14) that the presence of a LHJ structure results in a higher measured device diffusion length compared to similar devices without the n_+-n or p_+-p contact. This work suggests again that the usual methods of determining device diffusion length must be critically reviewed in light of the carrier accumulation (or blocking) property of the LHJ. Furthermore, the effect of finite sample dimensions, particularly as regards the influence of surface effects on the bulk diffusion length must also be considered when interpreting a diffusion length measurement.

Let us now turn our attention to other features of the LHJ model which are useful for interpreting the experimental results. The LHJ model appears to have wide applicability and permits a degree of insight into the influence of fabrication methods on cell performance. For example, the LHJ model has been applied to the pre- and post-irradiation performance of the epitaxial solar cell (15) with considerable success. In addition, the predicted radiation performance of thick and thin BSF cells, shown in fig. 8, are also in reasonable agreement with measured trends.

It is known that not all cells fabricated using the BSF process exhibit the high performance. The LHJ model via the parameter S (equation (5b)) suggests that in some cases the low voltages may be traced to

an imperfect LH barrier (N_A/N_{A+}) and undesirable p^+ region properties (width and diffusion length) both of which can result in large S values. The parameter S can be interpreted as a dimensionless quantity related to leakage of minority carriers in the p-region across the LH barrier into the p^+ side. The greater this leakage is, the larger the magnitude of S. This leakage is influenced by at least the following three effects: 1) a poor quality LHJ due to a diffusion anomaly, 2) an undesirable diffusion velocity (D/L) ratio, and 3) a small p^+ region W/L ratio. The first effect may arise from crystalline imperfections which enhance metallic precipitation and impurity spiking. In addition the alloying or diffusion process may be critically dependent on crystalline perfection and the presence of impurities which in turn would influence the p^+ region thickness and the carrier lifetime. Small values of the p^+ region W/L ratio can cause substantial increases in S even though the N_A/N_{A+} ratio may be desirably small and the p-region diffusion length relatively large. The consequence of these effects is that the cell would behave as if it had an ohmic rear contact, and hence yield voltages approaching those of the conventional cell.

In addition to the quality, the uniformity of the low-high junction must also influence cell performance. The effect of localized regions of the LHJ having widely different N_A/N_{A+} ratios, for example, is not known. This is true not only for the influence on V_{oc} but also on the measured cell diffusion length.

SUMMARY AND CONCLUSIONS

The open circuit voltage as a function of cell thickness has been calculated using the diode saturation current expressions appropriate to several solar cell structure models. Expressions were derived for the diode saturation currents appropriate to the drift field model and a new model proposed here, the low-high junction model. Also investigated were the infinite and finite base width cases of conventional cell model. In the latter, the zero and infinite surface recombination velocity approximations were considered. Comparisons were made with experimental data for back surface field (BSF) and conventional cells. The low-high junction model was compared to the experimental data for an unirradiated cell and cells irradiated with 1 MeV electrons.

Based on these analyses the following conclusions are made:

1. The zero SRV case of the conventional cell model, the drift field model, and the LHJ model can predict the high voltages measured in BSF cells. High voltages are predicted only when the W/L ratio of the p-base is less than unity However only the drift field and LHJ models describe cell performance in terms of parameters that are traceable to the fabrication process.

2. Based on the results of calculations, and the present lack of experimental data, no clear choice can be made as to which model is more appropriate for the high voltage BSF cell.

3. Calculated voltage degradation due to 1 MeV electron bombardment was compared with a limited amount of experimental data. The experimental trends of voltage degradation with cell thickness was predicted.

4. The p-base diffusion lengths required in the drift field and LHJ models of the high voltage cell are about 2 to 3 times higher than those required in the infinite SRV case applied to the conventional solar cell. The requirement of a high diffusion length poses an unresolved dilemma which suggest a further exploration of the factors that influence diffusion length.

5. The LHJ has been applied to the epitaxial solar cell and successfully predicts the measured trends.

APPENDIX

DERIVATION OF I_o FOR THE LOW-HIGH JUNCTION MODEL OF THE BSF SOLAR CELL

The cross section of a solar cell with a low-high junction as the rear contact is shown in fig. 9. The derivation of the saturation current for this cell structure begins with the following equations basic to any semiconductor device analysis:

Continuity Equations

$$\frac{dn}{dt} = G_n - R_n + \frac{1}{q}\nabla \cdot Jn \qquad \text{electrons} \qquad (1A)$$

$$\frac{dp}{dt} = G_p - R_p - \frac{1}{q}\nabla \cdot Jp \qquad \text{holes} \qquad (2A)$$

Current Transport Equations

$$J_n = q\mu_n nE + qD_n \nabla n \qquad \text{electrons} \qquad (3A)$$

$$J_p = q\mu_p pE - qD_p \nabla p \qquad \text{holes} \qquad (4A)$$

Poisson Equation

$$\nabla \cdot \bar{E} = \frac{q}{\epsilon\epsilon_o}(p - n + N_D - N_A) \qquad (5A)$$

where

$$E = -\nabla \Psi \qquad (6A)$$

Equations (1A) to (4A) may be combined following van Roosbroeck (16) to give the ambipolar continuity equation assuming space charge neutrality (i.e., $\Delta n = \Delta p$)

$$\frac{d\Delta n}{dt} = G_n - R_n + \mu^* E \nabla(\Delta n) + D^* \nabla^2(\Delta n) \qquad (7A)$$

where

$$\mu^* \text{ ambipolar mobility } \frac{p - n}{p/\mu_n + n/\mu_p} \qquad (8A)$$

$$D^* \text{ ambipolar diffusivity } \frac{p + n}{p/\mu_n + n/\mu_p} \qquad (9A)$$

For extrinsic material $\mu^* \cong \mu_n$ and $D^* \cong D_n$ and equation (7A) reduces to the more familiar expression describing continuity of minority carrier transport

$$\frac{d\Delta n}{dt} = G_n - R_n + \mu_n E \nabla(\Delta n) + D_n \nabla^2(\Delta n) \qquad (10A)$$

A more general statement of (10A) can be written assuming that not only the carrier density but also the mobility and the impurity concentrations are spatially dependent. Using equation (1A) to (5A) again, this equation has the form, for no external carrier generation and a steady state mode of operation

$$\nabla^2 n + \left(\frac{qE}{kT} + \frac{\nabla \cdot \mu_n}{\mu_n}\nabla n\right) + \left(\frac{qE}{kT}\frac{\nabla \cdot \mu_n}{\mu_n} + \nabla \cdot \frac{qE}{kT} - \frac{1}{L_n^2}\right) n + 0 \qquad (11A)$$

It should be recognized that in this case an effective electric field $\bar{E}$ is defined by

$$\frac{qE}{kT} + \frac{\nabla\mu_n}{\mu_n} \equiv \bar{E}$$

and an effective diffusion length $\bar{L}$ by

$$\frac{qE}{kT}\frac{\nabla\cdot\mu_n}{\mu_n} + \nabla\cdot\frac{qE}{kT} - \frac{1}{L_n^2} \equiv \frac{1}{\bar{L}^2}$$

In the field free case assuming a homogeneous material equation (11A) reduces to the simple form for low injection

$$\nabla^2 n - \frac{n}{L_n} = 0 \qquad (12A)$$

This equation has the general solution

$$n(x) = A\cosh x + \beta \sinh x \qquad (13A)$$

In applying this solution to the p-base solar cell containing a high low junction the following boundary conditions are employed

A. $x = x_j, n = n_{po}(\exp \beta V - 1)$ --- junction edge

B. $x = X, n_p(X) = n_{p+}(X)\exp \beta \psi_{LH}$ --- subregion boundary

$$qD_p\nabla n_p(X) = qD_{p+}\nabla n_{p+}(X)$$

C. $x = W, qD_{p+}\nabla n_{p+}(W) = -q s n_{p+}(W)$ --- metal - p^+ interface

Boundary condition B is of prime importance since it contains the potential barrier ψ_{LH} associated with the high-low junction and expresses the minority carrier concentrations at the space charge edges. The condition for current transport across the x = X boundary assumes that space charge recombination is negligible and that current is primarily by diffusion processes. This has been implied by equation (12A). Any excess minority carriers appearing at the p^+ region space charge edge as a result of the biasing of the n^+ p junction are assumed to diffuse to the metal rear contact. The recombination of the excess carriers there is controlled by the surface recombination velocity, s.

The solution for the excess minority carrier concentration for the one dimensional case is derived by dividing the p-region into two subregions the p-base and the p^+ base. The subregion boundary occurs at x = X. Both regions are assumed homogeneously doped, having acceptor concentrations N_A and N_{A+}. In addition the two regions are assumed to have different values of carrier lifetime and mobility. The general solutions for the p-base and p^+ region are

$$n_p(s) = A_1 \cosh x + B_1 \sinh x \qquad x_j \le x \le X$$

$$n_{p_+}(x) = A_2 \cosh x + B_2 \sinh x \qquad X \le x \le W$$

Application of the boundary conditions results in four equations and four unknowns.

Solving for the unknown coefficients results in the following solution for the excess carriers in the p-base

$$n_p(x) = n\,\frac{\cosh\frac{X-x}{L_p} + S\sinh\frac{X-x}{L_p}}{\cosh\frac{X}{L_p} + S\sinh\frac{X}{L_p}} \qquad (14A)$$

where S is defined as a normalized recombination velocity and is given by the following expression

$$S = \frac{N_A}{N_{A+}}\frac{D_{p+}}{D_p}\frac{L_p}{L_{p+}}\left\{\frac{\frac{s_r L_{p+}}{D_{p+}} + \tanh\frac{W_{p+}}{L_{p+}}}{1 + \frac{s_r L_{p+}}{D_{p+}}\tanh\frac{W_{p+}}{L_{p+}}}\right\} \qquad (15A\text{-}1)$$

where $W_{p+} = W - X$

As can be seen the parameter S not only describes the influence of the low-high junction by the N_A/N_{A+} ratio but also includes the p^+ region geometry factor in the bracket and the mobility and diffusion length associated with the two p regions. If it is assumed that an ohmic contact is made to the p^+ region, then the expression for S can be simplified to

$$\frac{N_A}{N_{A+}}\frac{D_{p+}}{D_p}\frac{L_p}{L_{p+}}\coth\frac{W_{p+}}{L_{p+}} \quad \text{for} \quad s \to \infty \qquad (15A\text{-}2)$$

In order to determine the diode saturation current, the gradient of excess carriers must be determined. This is obtained by differentiating equation (14A). Hence

$$\frac{dn(x)}{dx} = -\frac{n}{L_p}\,\frac{\sinh\frac{X-x}{L_p} + S\cosh\frac{X-x}{L_p}}{\cosh\frac{X}{L_p} + S\sinh\frac{X}{L_p}} \qquad (16A)$$

The diffusion current is obtained by evaluating the gradient at x = 0;

$$J_p = (-q)\,D_n\left.\frac{dn}{dx}\right|_{x=x_j}$$

This yields for the p-base component of the diffusion current

$$J_p = \frac{qD_n n_i^2}{N_A L_p}\left\{\frac{S + \tanh\frac{W_p}{L_p}}{1 + S\tanh\frac{W_p}{L_p}}\right\}(\exp \beta V - 1) \qquad (17A)$$

or

$$J_p = I_{p_o}(\exp \beta V - 1)$$

The expression for the p-base diode saturation is

$$I_{o_p} = \frac{qD_n n_i^2}{N_A L_p}\left\{\frac{S + \tanh\frac{W_p}{L_p}}{1 + S\tanh\frac{W_p}{L_p}}\right\} \qquad (18A)$$

This can be expressed in terms of total cell thickness by recognizing that $W_p = t - W_{n+} - (W_{p+})$ where W_{n+} and W_{p+} are the n^+ diffused region and p^+ layer thicknesses.

Since the total diode saturation current is composed of the n-layer and p-base contributions, an expression for the n-layer is needed. Either of three expressions may be appropriate depending on the particular model for the diffused layer. The n-layer may be viewed as a uniformly doped region of finite thickness W_{n+} bounded by the space charge layer on the one side and a metal contact of surface recombination velocity s on the other. For this case

$$I_{o_n} = \frac{qn_i^2 D_p}{N_D L_p} \left\{ \frac{\frac{s_f L_p}{D_n} + \tanh \frac{W_{n+}}{L_n}}{1 + \frac{s_f L_n}{D_n} \tanh \frac{W_{n+}}{L_n}} \right\} \qquad (19A)$$

If the n^+ layer is inhomogeneously doped the drift field model should be used. Should a low high junction model be used than an expression similar to equation (17A) can be derived.

However, it will be assumed for the purpose of this study that the diffused region contribution is always at least three orders of magnitude smaller that of the p-base. Simple calculations show this to be true assuming a homogeneous donor distribution of about 10^{17} to 10^{18}/cc. Therefore the total diode saturation current can be approximated by (18A) alone.

If it is assumed that diffusion transport processes are dominant in a solar cell operating at open circuit voltage, then the V_{oc} can be related to the saturation by the expression

$$V_{oc} = \frac{kT}{q} \ln \left(\frac{I_{sc}}{I_{o_p}} + 1 \right) \qquad (20A)$$

This equation together with (18A) is used in the study where $I_{o_n} = 5 \times 10^{-14}$ amp/cm^2 and $I_{sc} = 40$ ma/cm^2.

REFERENCES

1. J. Mandelkorn and J. H. Lamneck, Jr., "Simplified Fabrication of Back Surface Electric Field Silicon Cells and Novel Characteristics of Such Cells" Proceedings of 9th Photovoltaic Specialists Conference, May 2-3, 1972.

2. M. Wolf, "Drift Fields in Photovoltaic Solar Energy Converter Cells," Proc. IEEE, vol. 51, p. 674, May 1963.

3. J. B. Gunn, "On Carrier Accumulation and Properties of Certain Semiconductor Junctions," J. Electron. Control, vol. 4, pp. 17-50, 1958.

4. R. W. Dutton and R. J. Whittier, "Forward Current-Voltage and Switching Characteristics of p+nn+ (Epitaxial) Diodes," IEEE Trans. on Electron Devices, vol. ED-16, p. 458, May 1969.

5. D. P. Lieb, B. D. Jackson, and C. D. Root, "Abrupt Junction Diode Theory," IRE Trans. on Electron Devices, vol. ED-9, p. 143, Mar. 1962.

6. J. P. McKelvey, Solid State and Semiconductor. New York: Harper and Row, 1966.

7. W. Shockley, "The Theory of p-n Junctions in Semiconductors and p-n Junction Transistors," Bell Syst. Tech. J., vol. 28, p. 435, 1949.

8. D. A. Kleinman, "Considerations on the Solar Cell," Bell Syst. Tech. J., vol. 40, p. 81, 1961.

9. M. P. Godlewski, C. R. Baraona, and H. W. Brandhorst, Jr., "Drift Field Model Applied to the Lithium Containing Solar Cell," 10th Photovoltaic Specialists Conference, Nov. 13-15, 1973.

10. Private communication, Dr. H. W. Brandhorst, Jr., NASA-Lewis Research Center.

11. R. G. Downing, J. R. Carter, Jr., and J. M. Denny, "The Energy Dependence of Electron Damage in Silicon," Proceedings of the 4th Photovoltaic Specialists Conference, Vol. I, A-5-1, 1964.

12. P. Iles, "Effects of Processing on the Carrier Lifetime in Silicon Solar Cells," Contractors Final Report, NAS3-15689, to be published.

13. W. Zimmerman, "Measurement of Spatial Variations of the Carrier Lifetime in Silicon Power Devices," Phys. Stat. Sol. (a), vol. 12, p. 671, 1972.

14. P. Rai-Choudhury, "Chemical Vapor Deposited Silicon and Its Device Applications," Semiconductor Silicon 1973. Edited by H. R. Huff and R. R. Burgess, Electrochemical Society, Inc., 1973.

15. H. W. Brandhorst, Jr., C. R. Baraona, and C. K. Swartz, "Performance of Epitaxial Back Surface Field Cells," 10th Photovoltaic Specialists Conference, Nov. 13-15, 1973.

16. W. van Roosbroeck, "Theory of Current-Carrier Transport and Photoconductivity in Semiconductors with Trapping," Bell Syst. Tech. J., vol. 39, pp. 515-613, May 1960.

EXPERIMENTAL THICKNESS-VOLTAGE PERFORMANCE OF
BSF AND CONVENTIONAL 10 OHM-CM CELLS

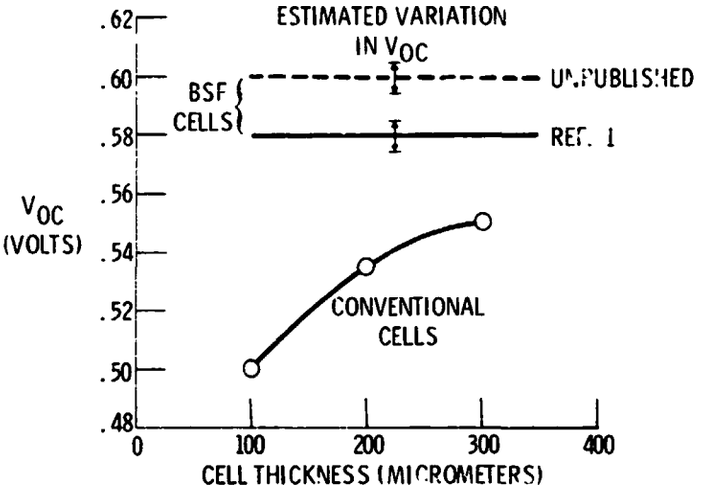

Fig. 1a

EXPERIMENTAL RADIATION DAMAGE - VOLTAGE PERFORMANCE
OF BSF AND CONVENTIONAL 10 OHM-CM CELLS

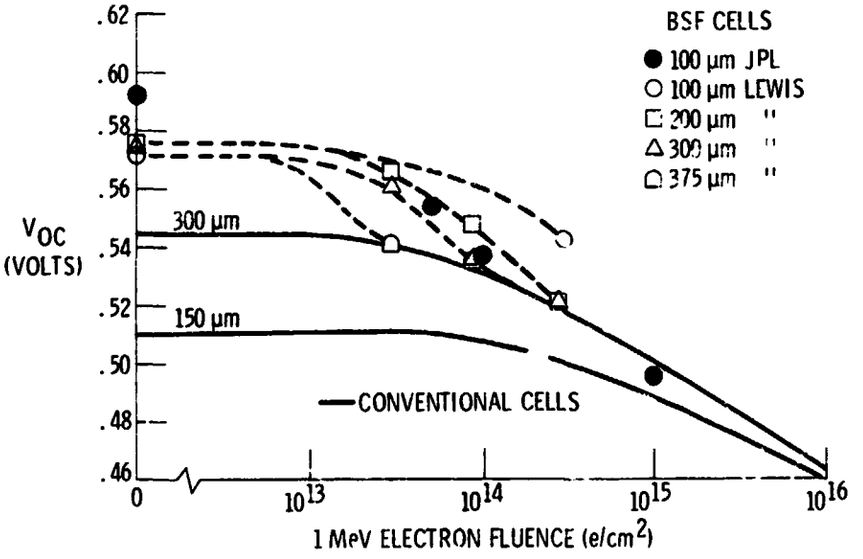

Fig. 1b

DEPENDENCE OF OPEN CIRCUIT VOLTAGE ON P-BASE
DIFFUSION LENGTH FOR INFINITE BASE WIDTH MODEL

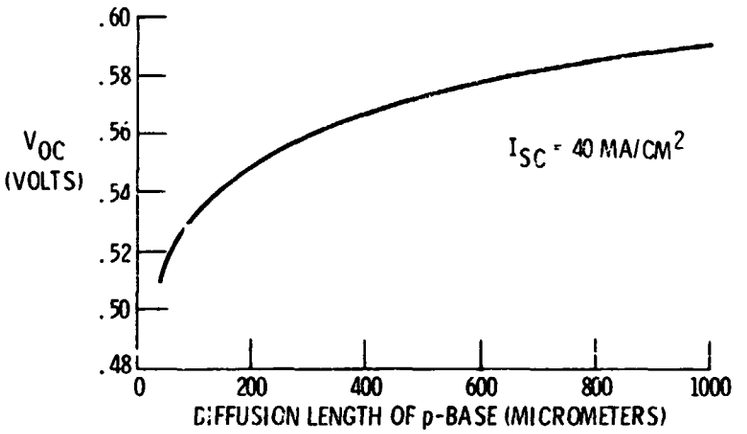

Fig. 2

DEPENDENCE OF OPEN CIRCUIT VOLTAGE ON CELL THICKNESS
FOR FINITE WIDTH MODEL

I_{SC} = 40 ma/cm^2, W_{p+} = 0.5 µm, L_{p+} = 1.0 µm, ρ_p = 10 Ω-cm

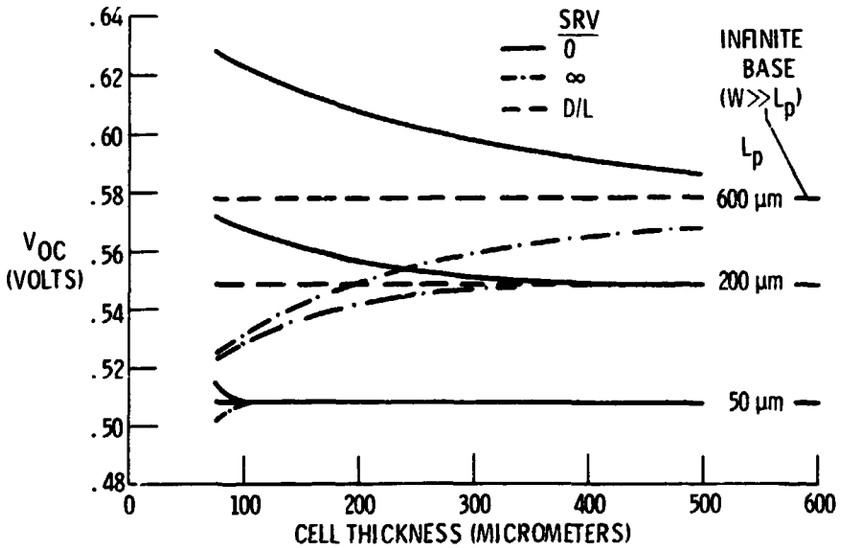

Fig. 3

DEPENDENCE OF OPEN CIRCUIT VOLTAGE ON CELL THICKNESS FOR DRIFT FIELD MODEL

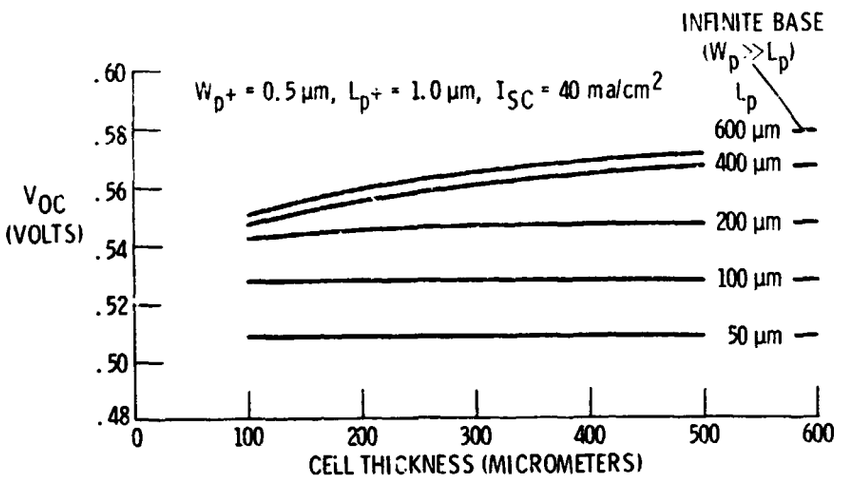

Fig. 4

E-7129

EFFECT OF P^+ REGION DIFFUSION LENGTH ON OPEN CIRCUIT VOLTAGE FOR DRIFT FIELD MODEL

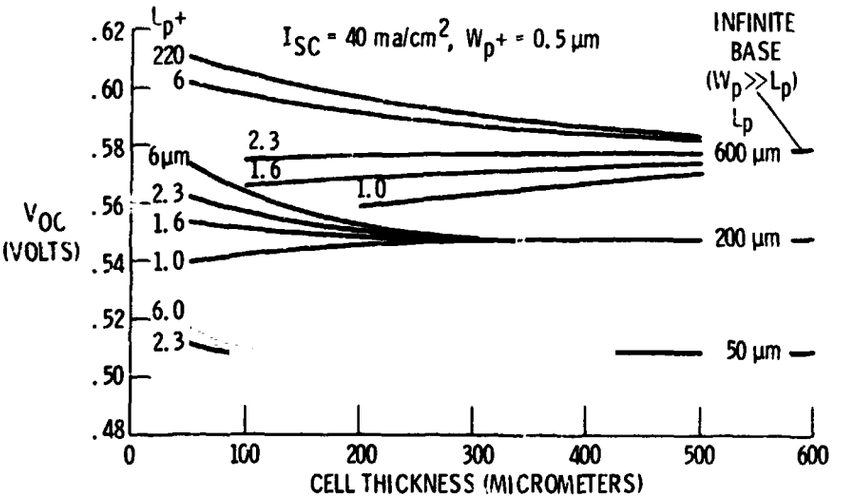

Fig. 5

DEPENDENCE OF OPEN CIRCUIT VOLTAGE ON CELL THICKNESS
FOR THE LOW-HIGH JUNCTION MODEL

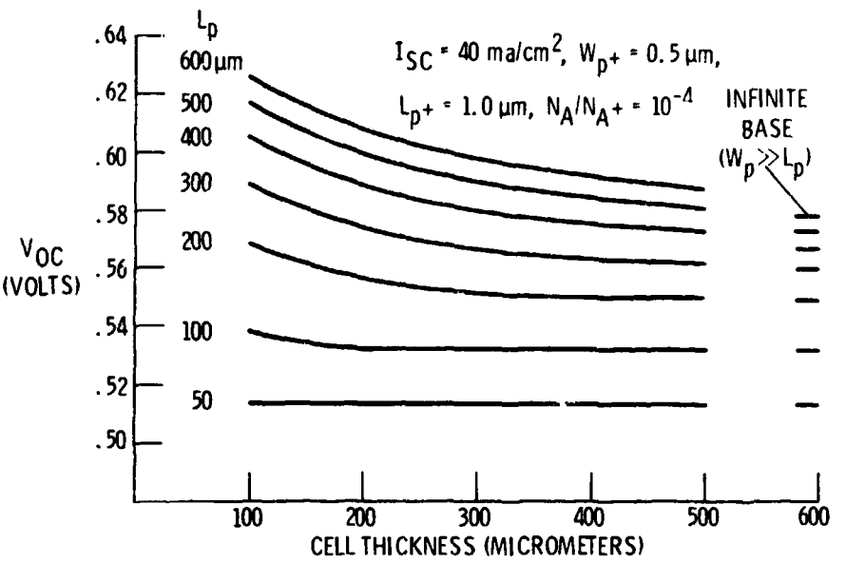

Fig. 6

DEPENDENCE OF OPEN CIRCUIT VOLTAGE ON NORMALIZED
SURFACE RECOMBINATION VELOCITY S

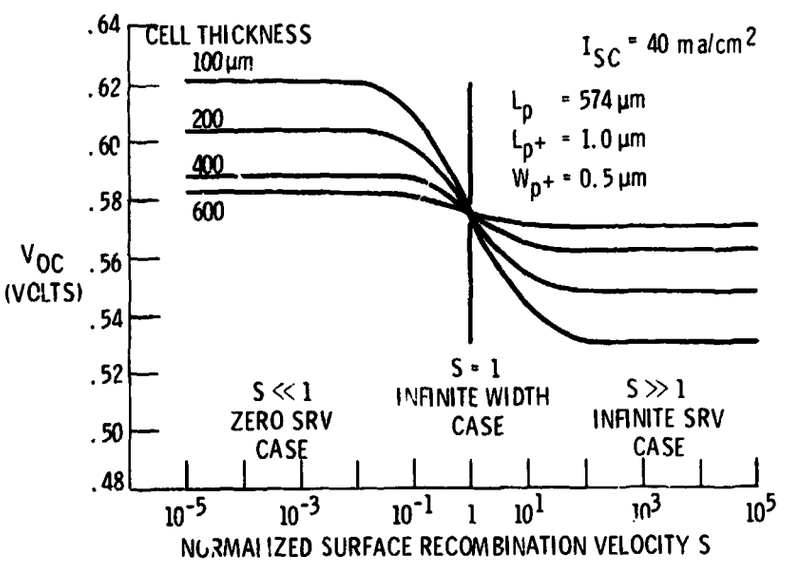

Fig. 7

CALCULATED RADIATION PERFORMANCE FOR
BSF AND CONVENTIONAL CELLS

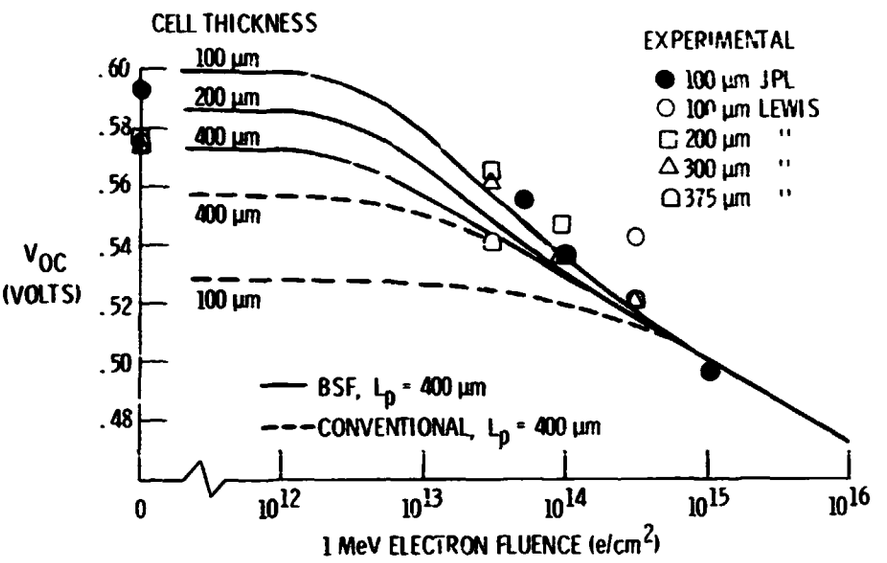

Fig. 8

E-7829

CROSS SECTION OF A SOLAR CELL WITH A LOW-HIGH JUNCTION
AS PART OF THE REAR CONTACT FOR A FIELD FREE CONDITION

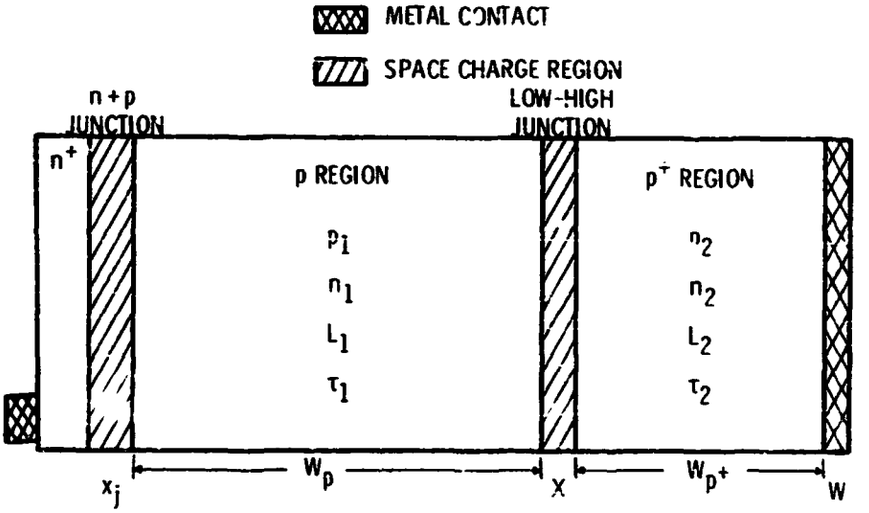

Fig. 9

NASA-Lewis